

Multi-photon-addition amplified coherent state

Xue-feng Zhan¹, Qiang Ke¹, Min-xiang Li², and Xue-xiang Xu^{1,†}

¹College of Physics and Communication Electronics,
Jiangxi Normal University, Nanchang 330022, China;

²School of Education, Jiangxi Normal University,
Nanchang 330022, China;

[†]xuxuexiang@jxnu.edu.cn

State $g^{\hat{n}}\hat{a}^{\dagger m}|\alpha\rangle$ and state $\hat{a}^{\dagger m}g^{\hat{n}}|\alpha\rangle$ are same to state $\hat{a}^{\dagger m}|g\alpha\rangle$, which is called as multi-photon-addition amplified coherent state (MPAACS) by us. Here, \hat{n} , \hat{a}^{\dagger} , $|\alpha\rangle$, g (≥ 1), and m are photon number operator, creation operator, coherent state, gain factor, and an interger, respectively. We study mathematical and physical properties for these MPAACSs, including normalization, photon component analysis, Wigner function, effective gain, quadrature squeezing, and equivalent input noise. Actually, the MPAACS, which contains more nonclassicality, is an amplified version of photon-added coherent state (PACS) introduced by Agrwal and Tara [Phys. Rev. A 43, 492 (1991)]. Our work provides theoretical references for implementing amplifiers for light fields.

Keywords: noiseless linear amplification; repeated photon addition; amplified coherent state; noise; Wigner function

I. INTRODUCTION

In physics, signal amplification is a simple concept. However, signal amplification unavoidably comes with noise[1]. Often, the introduced noise makes it difficult for people to distinguish the amplified signal. The downside is that quantum noise will restrict quantum technologies such as quantum cloning[2, 3] and superluminal information transfer[4]. In order to conquer this restriction, people are more looking forward to taking advantage of noiseless amplification, which can be implemented by probabilistic operations[5, 6]. In recent years, the theoretical and experimental study on ideal noiseless linear amplification (NLA) has attracted the interests of the researchers[7–10]. The NLA has been used for many quantum information tasks such as loss suppression[11], quantum repeater[12], quantum error correction[13], and entanglement distillation[14].

The NLA can be described by the operator $g^{\hat{n}}$ (AM), where $\hat{n} = \hat{a}^{\dagger}\hat{a}$ is the photon number operator and g ($g > 1$) is the gain factor. Here $g^{\hat{n}} \equiv \hat{1}$ is just the identity operator if $g = 1$. The NLA can be implemented probabilistically by combining multiple photon addition and subtraction with current technology[15]. Theoretically, an ideal noiseless amplifier (described by $g^{\hat{n}}$) can map an input state ρ_{in} into an output state ρ_{out} , i.e., $g^{\hat{n}} : \rho_{in} \mapsto \rho_{out}$. For input Fock state $|n\rangle$, we have $g^{\hat{n}} : |n\rangle \mapsto |n\rangle$ due to $\hat{n}|n\rangle = n|n\rangle$. For input coherent state (CS), we have $g^{\hat{n}} : |\alpha\rangle \mapsto |g\alpha\rangle$ because of $g^{\hat{n}}|\alpha\rangle = e^{(g^2-1)|\alpha|^2/2}|g\alpha\rangle$. Generally, the input states to be amplified by $g^{\hat{n}}$ include Gaussian and non-Gaussian state[16]. Moreover, the output states must be re-normalized after operating $g^{\hat{n}}$ because this operator is unbounded.

In 2016, Park et al. suggested and compared several schemes for non-deterministic NLA of CSs using $\hat{a}^{\dagger 2}$, $\hat{a}\hat{a}^{\dagger}$, $(\hat{a}\hat{a}^{\dagger})^2$, $\hat{a}^{\dagger 4}$, $\hat{a}\hat{a}^{\dagger}\hat{a}^{\dagger 2}$, $\hat{a}^{\dagger 2}\hat{a}\hat{a}^{\dagger}$, which may work as amplifiers for CSs with weak, medium or large amplitudes. Among

them, the two-photon addition ($\hat{a}^{\dagger 2}$) scheme work more effectively than others as a noiseless amplifier[17]. Before then, in 1991, Argarwal and Tara had introduced photon-added CSs (PACS) $\hat{a}^{\dagger m}|\alpha\rangle$, which can be generated by applying a m -photon addition $\hat{a}^{\dagger m}$ (AD) on the CS $|\alpha\rangle$, where m is an interger[18]. It is undeniable that the AD $\hat{a}^{\dagger m}$ also works as an amplifier to amplify $|\alpha\rangle$ to $\hat{a}^{\dagger m}|\alpha\rangle$.

In this paper, we shall study the behaviour of $\hat{a}^{\dagger m}|\alpha\rangle$ under the action of $g^{\hat{n}}$. In another words, we shall obtain new quantum states by further applying $g^{\hat{n}}$ on $\hat{a}^{\dagger m}|\alpha\rangle$. We will analyze their nonclassical properties and amplification effects. The key is to examine the combinatorial effects of AD $\hat{a}^{\dagger m}$ and AM $g^{\hat{n}}$ on CSs. The remaining paper is organized as follows. In Sec.2, we introduce our considered states accompanying with description and normalization. In Sec.3, we analyze photon components for them. In Sec.4, we study Wigner functions to show character of Gaussianity and nonclassicality. Sec.5 is devoted to studying effective gain, quadrature squeezing and equivalent input noise for these states. Conclusions are summarized in the last section.

II. GENERATING QUANTUM STATES

Based on operators $g^{\hat{n}}$, $\hat{a}^{\dagger m}$, and CS $|\alpha\rangle$, we introduce a class of new states by two equivalent ways. The conceptual generating schemes are shown in Fig.1.

Way 1: Employing $\hat{a}^{\dagger m}$ then $g^{\hat{n}}$ on $|\alpha\rangle$, we get the addition-amplification coherent state (ADAMCS)

$$|\psi_1\rangle = \frac{1}{\sqrt{N_1}}g^{\hat{n}}\hat{a}^{\dagger m}|\alpha\rangle, \quad (1)$$

with normalization factor

$$N_1 = g^{2m}m!e^{(g^2-1)|\alpha|^2}L_m(-g^2|\alpha|^2), \quad (2)$$

where $L_m(x)$ is the m th-order Laguerre polynomial[19]. This map include two processes, i.e., $\hat{a}^{\dagger m} : |\alpha\rangle \mapsto$

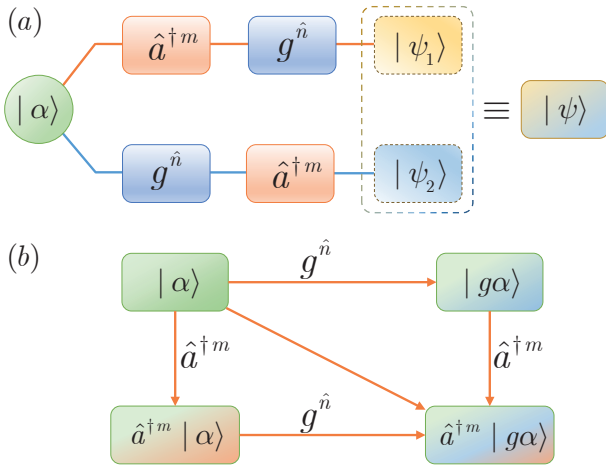


FIG. 1: (a) Conceptual generating schemes of ADAMCS $|\psi_1\rangle$ and AMADCS $|\psi_2\rangle$. It is interesting to prove that $|\psi_1\rangle$ and $|\psi_2\rangle$ are the same MPAACS $|\psi\rangle$. (b) The map $|\alpha\rangle \mapsto \hat{a}^{\dagger m} |g\alpha\rangle$ can be implemented by way 1 $|\alpha\rangle \mapsto \hat{a}^{\dagger m} |\alpha\rangle \mapsto \hat{a}^{\dagger m} |g\alpha\rangle$ or by way 2 $|\alpha\rangle \mapsto |g\alpha\rangle \mapsto \hat{a}^{\dagger m} |g\alpha\rangle$ after employing $g^{\hat{n}}$ and $\hat{a}^{\dagger m}$ in sequence.

$\hat{a}^{\dagger m} |\alpha\rangle$ and $g^{\hat{n}} : \hat{a}^{\dagger m} |\alpha\rangle \mapsto |\psi_1\rangle$, where $\hat{a}^{\dagger m} |\alpha\rangle$ is the intermediate state.

Way 2: Employing $g^{\hat{n}}$ then $\hat{a}^{\dagger m}$ on $|\alpha\rangle$, we get the amplification-addition coherent state (AMADCS)

$$|\psi_2\rangle = \frac{1}{\sqrt{N_2}} \hat{a}^{\dagger m} g^{\hat{n}} |\alpha\rangle, \quad (3)$$

with normalization factor

$$N_2 = m! e^{(g^2-1)|\alpha|^2} L_m(-g^2|\alpha|^2). \quad (4)$$

This map include two processes, i.e., $g^{\hat{n}} : |\alpha\rangle \mapsto |g\alpha\rangle$ and $\hat{a}^{\dagger m} : |g\alpha\rangle \mapsto |\psi_2\rangle$, where $|g\alpha\rangle$ is the intermediate state.

Although operators $g^{\hat{n}}$ and $\hat{a}^{\dagger m}$ do not commute with each other (i.e. $g^{\hat{n}} \hat{a}^{\dagger m} \neq \hat{a}^{\dagger m} g^{\hat{n}}$), the relation $g^{\hat{n}} \hat{a}^{\dagger m} = g^m \hat{a}^{\dagger m} g^{\hat{n}}$ is satisfied and leads to $|\psi_1\rangle = |\psi_2\rangle$ after normalization. Thus, we redefine them as $|\psi\rangle$ in the form

$$|\psi\rangle = \frac{1}{\sqrt{N}} \hat{a}^{\dagger m} |g\alpha\rangle, \quad (5)$$

with normalization factor $N = m! L_m(-g^2|\alpha|^2)$. In this paper, we call $|\psi\rangle$ as MPAACS, which is just an amplified PACS. By using $|\psi_1\rangle$ in Appendix A or by using $|\psi_2\rangle$ in Appendix B in two parallel ways, we get the expressions of state description, normalization factor, expectation value, density matrix elements, and Wigner function for $|\psi\rangle$. Without question, the results in Appendix A are same to those in Appendix B except $N_1 = g^{2m} N_2$. As illustrated in Table I, states including $|0\rangle$, $|m\rangle$, $|\alpha\rangle$, $|g\alpha\rangle$, and $\hat{a}^{\dagger m} |\alpha\rangle$ are special cases of $|\psi\rangle$ with proper g , α , and m .

TABLE I: Special cases of the MPAACS

$ \psi\rangle$	parameter conditions	state name
$ 0\rangle$	$m = 0, \alpha = 0$	vacuum state
$ m\rangle$	$\alpha = 0$	Fock state
$ \alpha\rangle$	$g = 1, m = 0$	coherent state
$ g\alpha\rangle$	$m = 0$	amplified CS
$\hat{a}^{\dagger m} \alpha\rangle$	$g = 1$	photon-added CS

III. COMPONENT ANALYSIS OF THE MPAACS

The MPAACS can be expanded in terms of Fock states as

$$|\psi\rangle = \sum_{k=m}^{\infty} c_k |k\rangle, \quad (6)$$

with

$$c_k = \frac{\sqrt{k!} (g\alpha)^{k-m} e^{-g^2|\alpha|^2/2}}{(k-m)! \sqrt{m! L_m(-g^2|\alpha|^2)}}. \quad (7)$$

It is interesting to note that the components including $|k\rangle$ ($k < m$) are missing in the MPAACS. Moreover, when $g = 1$, the result can be reduced to that in the work of Agarwal and Tara[18]. Accordingly, the density matrix element (DME) for $\rho = |\psi\rangle \langle\psi|$ can be expressed as $\rho_{kl} = \langle k|\rho|l\rangle = c_k c_l^*$, whose numerical results also can be calculated according to Eq.(A.7) or Eq.(B.6) in the Appendix. The photon number distribution (PND) can be written as $\rho_{kk} = |c_k|^2$, i.e., the diagonal terms of the density matrix. Without loss of generality, we shall take $\alpha = |\alpha| e^{i\theta_p}$ only with $\theta_p = 0$ in the numerical analysis.

Fig.2 presents the PNDs ρ_{kk} of the MPAACSs with different parameters ($|\alpha|, g, m$). The results show that: (a) The effect of photon-added number m can be observed in Fig.2(a) at fixed $|\alpha| = 1, g = 2$ and for three different m . As m increases, the PNDs ρ_{kk} approach higher-photon regime where all the $|k\rangle$ terms with $k < m$ are missing, like a shifted version of original amplified CS ($m = 0$). (b) The effect of gain factor g can be observed in Fig.2(b) at fixed $|\alpha| = 1, m = 2$ and for three different g . It is obvious to see that the PNDs approach higher-photon regime as g increasing. (c) The effect of the field amplitude $|\alpha|$ can be observed in Fig.2(c) at fixed $g = 2, m = 2$ and for three different $|\alpha|$. We find if $|\alpha| = 0$, there is the sole component of $|m\rangle$. If case $|\alpha| > 0$, the PNDs approach higher-photon regime as $|\alpha|$ increasing.

Fig.3 presents the absolute values of the DMEs ($|\rho_{kl}|$) of the MPAACSs showing the effects of parameters ($|\alpha|, g, m$). Generally, two adjacent states, corresponding to two adjacent graphs in Fig.3, can be connected through a map with its operation. These maps include $\hat{a}^{\dagger m} : |0\rangle \mapsto |m\rangle$ for (a)-(b); $D(\alpha) : |0\rangle \mapsto |\alpha\rangle$ for (a)-(c), where

$D(\alpha) = e^{\alpha a^\dagger - \alpha^* a}$ is the displacement operator; $\hat{a}^{\dagger m} : |\alpha\rangle \mapsto \hat{a}^{\dagger m} |\alpha\rangle$ for (c)-(d); $g^{\hat{n}} : |\alpha\rangle \mapsto |g\alpha\rangle$ for (e); $g^{\hat{n}} : \hat{a}^{\dagger m} |\alpha\rangle \mapsto \hat{a}^{\dagger m} |g\alpha\rangle$ for (d)-(f); $\hat{a}^{\dagger m} : |g\alpha\rangle \mapsto \hat{a}^{\dagger m} |g\alpha\rangle$ for (e)-(f). Of course, the map $|m\rangle \mapsto \hat{a}^{\dagger m} |\alpha\rangle$ for (b)-(d) can not be realized simply by $D(\alpha)$. It can be easily seen from Fig.3 that: (1) The AD $\hat{a}^{\dagger m}$ leads to the rescale of corresponding DMEs and the displacement to higher indices ($\rho_{k,l} \rightarrow \rho_{k+m,l+m}$), leaving all $\rho_{k,l}$ with $k, l < m$ void. (2) The AM $g^{\hat{n}}$ leads to the rescale of corresponding DMEs.

IV. WIGNER FUNCTION OF THE MPAACS

In phase-space formalism, the Wigner function (WF) is an important quasiprobability distribution, representing the corresponding quantum state[20–22]. One can judge Gaussianity or non-Gaussianity from its WF form and non-classicality from its Wigner negativity[23, 24]. Theoretically, $W_\rho(\beta)$ can be also obtained by means of the following transformation

$$W_\rho(\beta) = \sum_{k,l=0}^{\infty} \rho_{kl} W_{|k\rangle\langle l|}(\beta) \quad (8)$$

which is associated with ρ_{kl} and $W_{|k\rangle\langle l|}(\beta)$ (WF of operator $|k\rangle\langle l|$). But it is very difficult to simulate perfectly as given by Eq.(8) because of the infinite summation. In experiment, the approximate WF can be reconstructed from a truncated density matrix with finite dimension through tomographic analysis.

Fortunately, analytical WF of the MPAACS can be obtained from Eq.(A.8) or Eq.(B.7) as follows

$$W_\rho(\beta) = \frac{2(-1)^m L_m(|2\beta - g\alpha|^2)}{\pi L_m(-g^2|\alpha|^2)} e^{-2|\beta - g\alpha|^2}, \quad (9)$$

in the (x, y) phase space, where $\beta = (x + iy)/\sqrt{2}$. As expected, Eq.(9) can reduce to the following special cases.

(1) If $\alpha = 0$ and $m = 0$, then we obtain WF of vacuum state

$$W_{|0\rangle}(\beta) = \frac{2}{\pi} e^{-2|\beta|^2}. \quad (10)$$

(2) If $m = 0$ and $g = 1$, then we obtain WF of coherent state

$$W_{|\alpha\rangle}(\beta) = \frac{2}{\pi} e^{-2|\beta - \alpha|^2}. \quad (11)$$

(3) If $m = 0$, then we obtain WF of amplified CS

$$W_{|g\alpha\rangle}(\beta) = \frac{2}{\pi} e^{-2|\beta - g\alpha|^2}. \quad (12)$$

(4) If $\alpha = 0$, then we obtain WF of Fock state

$$W_{|m\rangle}(\beta) = \frac{2}{\pi} (-1)^m e^{-2|\beta|^2} L_m(4|\beta|^2). \quad (13)$$

(5) If $g = 1$, then we obtain WF of photon-added CS

$$W_{\hat{a}^{\dagger m}|\alpha\rangle}(\beta) = \frac{2(-1)^m L_m(|2\beta - \alpha|^2)}{\pi L_m(-|\alpha|^2)} e^{-2|\beta - \alpha|^2}. \quad (14)$$

Eq.(14) is just the equation (3.8) in Ref.[18].

Corresponding to Fig.3 and according to Eqs.(9)-(14), we plot WFs in Fig.4 and their sections (with $y = 0$) in Fig.5(a), as well as their marginal distributions in Fig.5(b). Here, the marginal distribution in x direction can be evaluated numerically by

$$p(x) = \int_{-\infty}^{\infty} W(\beta) dy, \quad (15)$$

where the scaling relations such as $\int_{-\infty}^{\infty} W(\beta) d^2\beta = 1$ and $\int_{-\infty}^{\infty} p(x) dx = 1$ must be ensured.

The left three figures of Fig.4 correspond to vacuum state $|0\rangle$, coherent state $|\alpha\rangle$, and amplified CS $|g\alpha\rangle$. Their distributions are Gaussian without Wigner negativity and with different central positions. The right three figures of Fig.4 correspond to Fock state $|m\rangle$, Photon-added CS $\hat{a}^{\dagger m}|\alpha\rangle$, and MPAACS $\hat{a}^{\dagger m}|g\alpha\rangle$. Their distributions are non-Gaussian and showing Wigner negativity. Main characters including Gaussianity (or non-Gaussianity) and nonclassicality (negativity) can also be seen from their corresponding sections in $y = 0$ in Fig.5(a). Moreover, we see from Fig.5(b) that, as m is increased, the width of distribution $p(x)$ becomes narrower comparing to that of $|\alpha\rangle$ and $|g\alpha\rangle$ (corresponding to $m = 0$) with $|\alpha| > 0$. We think, this is owe to the effect of AD $\hat{a}^{\dagger m}$.

V. EFFECTIVE GAIN, QUADRATURE SQUEEZING AND EQUIVALENT INPUT NOISE

Generally, many properties of light states are related to amplitude quadrature $\hat{x} = (a + a^\dagger)/\sqrt{2}$ and phase quadrature $\hat{p} = (a - a^\dagger)/(i\sqrt{2})$ [25, 26]. In order to study the combinatorial contributions of AM $g^{\hat{n}}$ and AD $\hat{a}^{\dagger m}$, we compare the properties of $|\alpha\rangle$ and $|\psi\rangle$ in terms of the effective gain, quadrature squeezing, and equivalent input noise. After our full consideration, we only use quadrature operator \hat{x} to discuss all these properties.

Effective gain: An effective gain[27, 28] from the input $|\alpha\rangle$ to the output $|\psi\rangle$ can be defined as the ratio of the expectation values of the quadrature operator \hat{x} :

$$g_{eff} = \frac{\langle \hat{x} \rangle_{|\psi\rangle}}{\langle \hat{x} \rangle_{|\alpha\rangle}}. \quad (16)$$

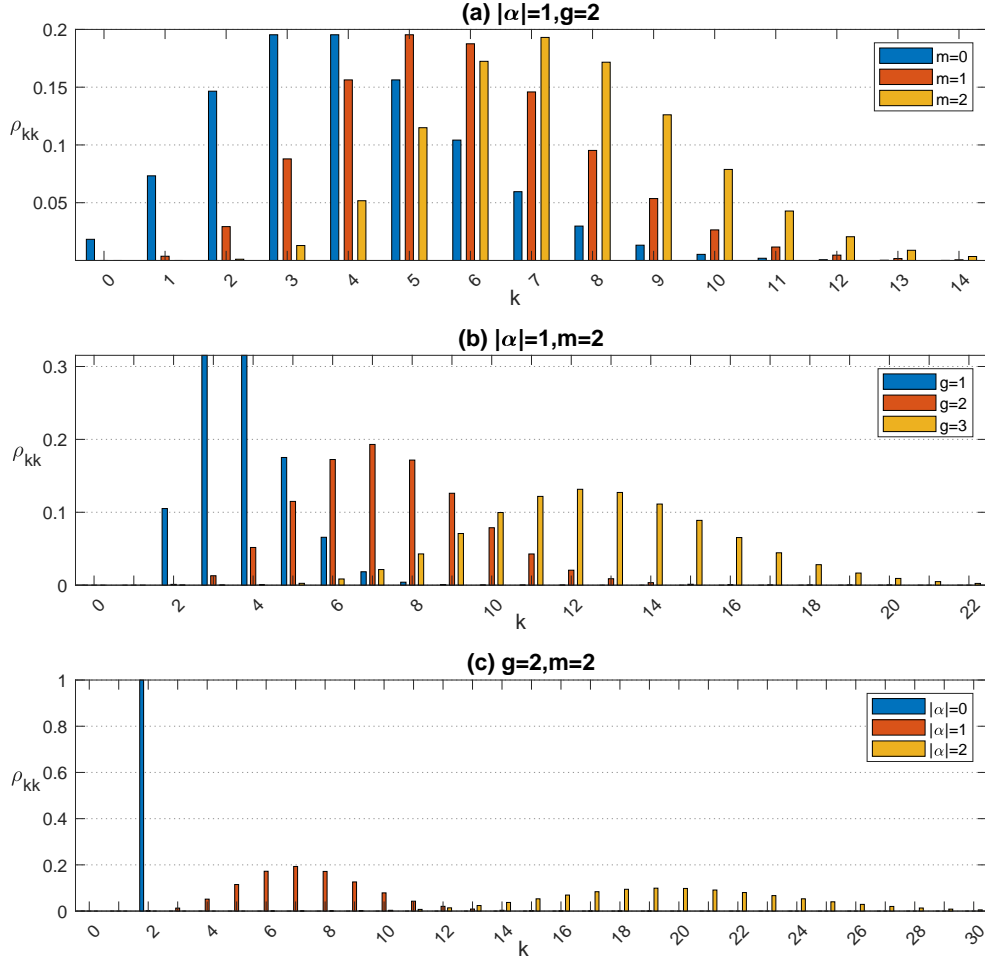


FIG. 2: PNDs of $|\psi\rangle$ with different $(|\alpha|, g, m)$. (a) showing the effect of m ; (b) showing the effect of g ; (c) showing the effect of $|\alpha|$.

In particularly, we have

$$\begin{aligned}
 g_{eff}^{(m=0)} &= g, \\
 g_{eff}^{(m=1)} &= g \frac{2 + g^2 |\alpha|^2}{1 + g^2 |\alpha|^2}, \\
 g_{eff}^{(m=2)} &= g \frac{6 + 6g^2 |\alpha|^2 + g^4 |\alpha|^4}{2 + 4g^2 |\alpha|^2 + g^4 |\alpha|^4}, \\
 &\vdots
 \end{aligned} \tag{17}$$

In Fig.6(a), we plot g_{eff} as a function of $|\alpha|$ by taking different g and m . From Fig.6(a), we find that $g_{eff} \gtrsim g$ is always right and g_{eff} is a monotonical decreasing function of $|\alpha|$ for different g and $m > 0$. Two limiting cases include: (1) $g_{eff} \rightarrow (m+1)g$ in the limit of $|\alpha| \rightarrow 0$; (2) $g_{eff} \rightarrow g$ in the limit of $|\alpha| \rightarrow \infty$.

Quadrature squeezing: Quadrature squeezing, as a

nonclassical character of light states, can be evident by measuring the quadrature variances[29, 30]. The quadrature variance in \hat{x} can be calculated from

$$\langle (\Delta \hat{x})^2 \rangle = \langle \hat{x}^2 \rangle - \langle \hat{x} \rangle^2, \tag{18}$$

which is also called as the quadrature fluctuation. Similar definition $\langle (\Delta \hat{p})^2 \rangle$ is available to quadrature \hat{p} . It is well known that $|\alpha\rangle$ and $|g\alpha\rangle$ are not quadrature squeezing states because of $\langle (\Delta \hat{x})^2 \rangle = \langle (\Delta \hat{p})^2 \rangle = 0.5$. While if $\langle (\Delta \hat{x})^2 \rangle$ or $\langle (\Delta \hat{p})^2 \rangle$ is smaller than 0.5, then the quantum state is quadrature squeezing. Thus, a question naturally arises: is the MPAACS quadrature squeezing? In order to answer this question, we only plot $\langle (\Delta \hat{x})^2 \rangle$ as a function of $|\alpha|$ for different $|\psi\rangle$ in Fig.6(b) regardless of

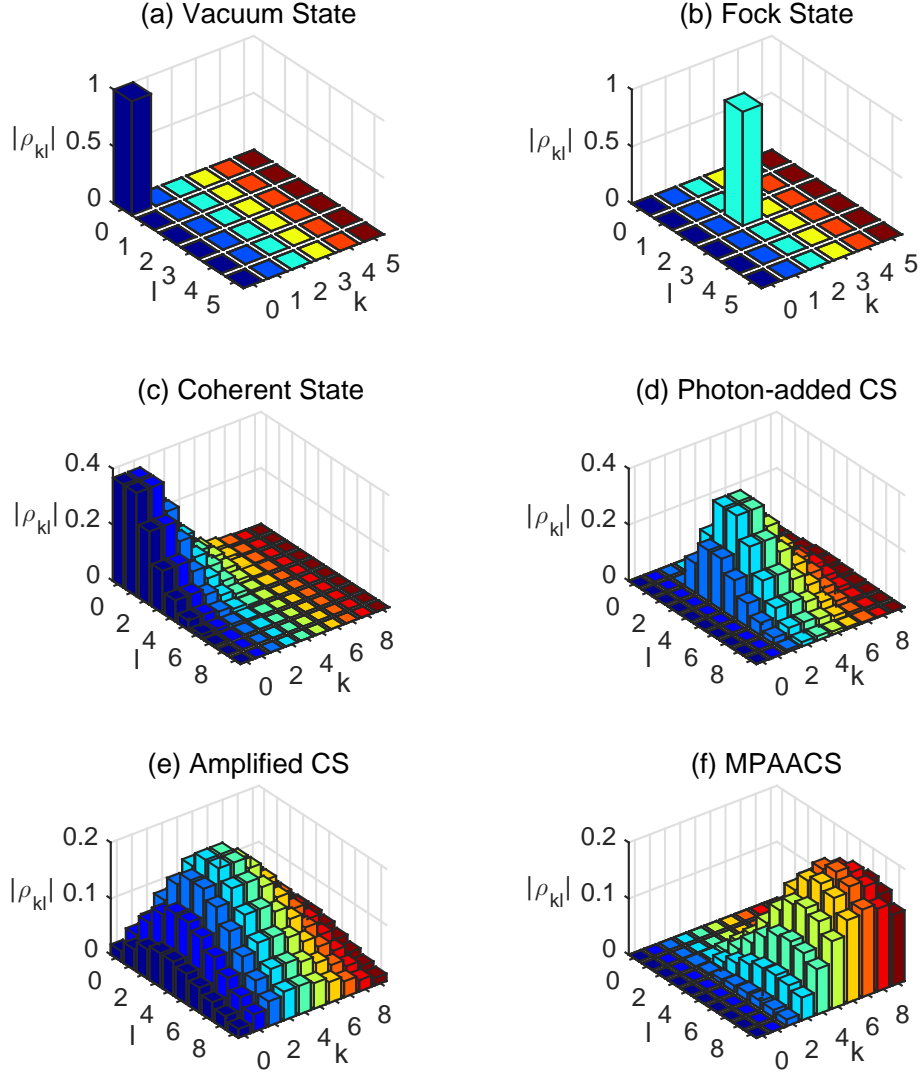


FIG. 3: Absolute values of DMEs for $|\psi\rangle$ - $(|\alpha\rangle, g, m)$ taking (a) $|0\rangle$ - $(0, 1, 0)$; (b) $|m\rangle$ - $(0, 1, 2)$; (c) $|\alpha\rangle$ - $(1, 1, 0)$; (d) $a^{\dagger m} |\alpha\rangle$ - $(1, 1, 2)$; (e) $|g\alpha\rangle$ - $(1, 2, 0)$; and (f) $a^{\dagger m} |g\alpha\rangle$ - $(1, 2, 2)$. Indeed, any two adjacent states can be connected through appropriate operations such as $D(\alpha)$, $a^{\dagger m}$, and $g^{\hat{n}}$.

$$\langle (\Delta \hat{p})^2 \rangle \geq 0.5.$$

Clearly, we find that (1) For $m = 0$ case, the \hat{x} quadrature variance remains constant fluctuation 0.5 (without quadrature squeezing) for any g and $|\alpha|$. This is because $|\psi\rangle$ has been reduced to $|\alpha\rangle$ or $|g\alpha\rangle$ in this case. (2) For $m = 1$ case, the \hat{x} quadrature exhibits squeezing if $|g\alpha| > 1$, which is consistent with the result for SPACS[31]. (3) For $m = 2$ case, the \hat{x} quadrature exhibits squeezing if $|g\alpha| > 0.938744$. Other similar reduced fluctuations will be exhibited squeezing if $|g\alpha| > 0.900407$ for $m = 3$, $|g\alpha| > 0.873904$ for $m = 4$, $|g\alpha| > 0.854454$ for $m = 5$,

and so on. (4) All above results show that the MPAACSS except $m = 0$ will exhibit quadrature squeezing, only when $|g\alpha|$ exceeds a certain threshold. (5) Moreover, we always have $\langle (\Delta \hat{x})^2 \rangle \rightarrow 0.5$ in the limit of $|\alpha| \rightarrow \infty$.

Equivalent input noise: Noise of the output $|\psi\rangle$ referring to the input $|\alpha\rangle$ may be analyzed in terms of the equivalent input noise (EIN):

$$N_{eq} = \frac{\langle (\Delta \hat{x})^2 \rangle_{|\psi\rangle}}{g_{eff}^2} - \langle (\Delta \hat{x})^2 \rangle_{|\alpha\rangle}, \quad (19)$$

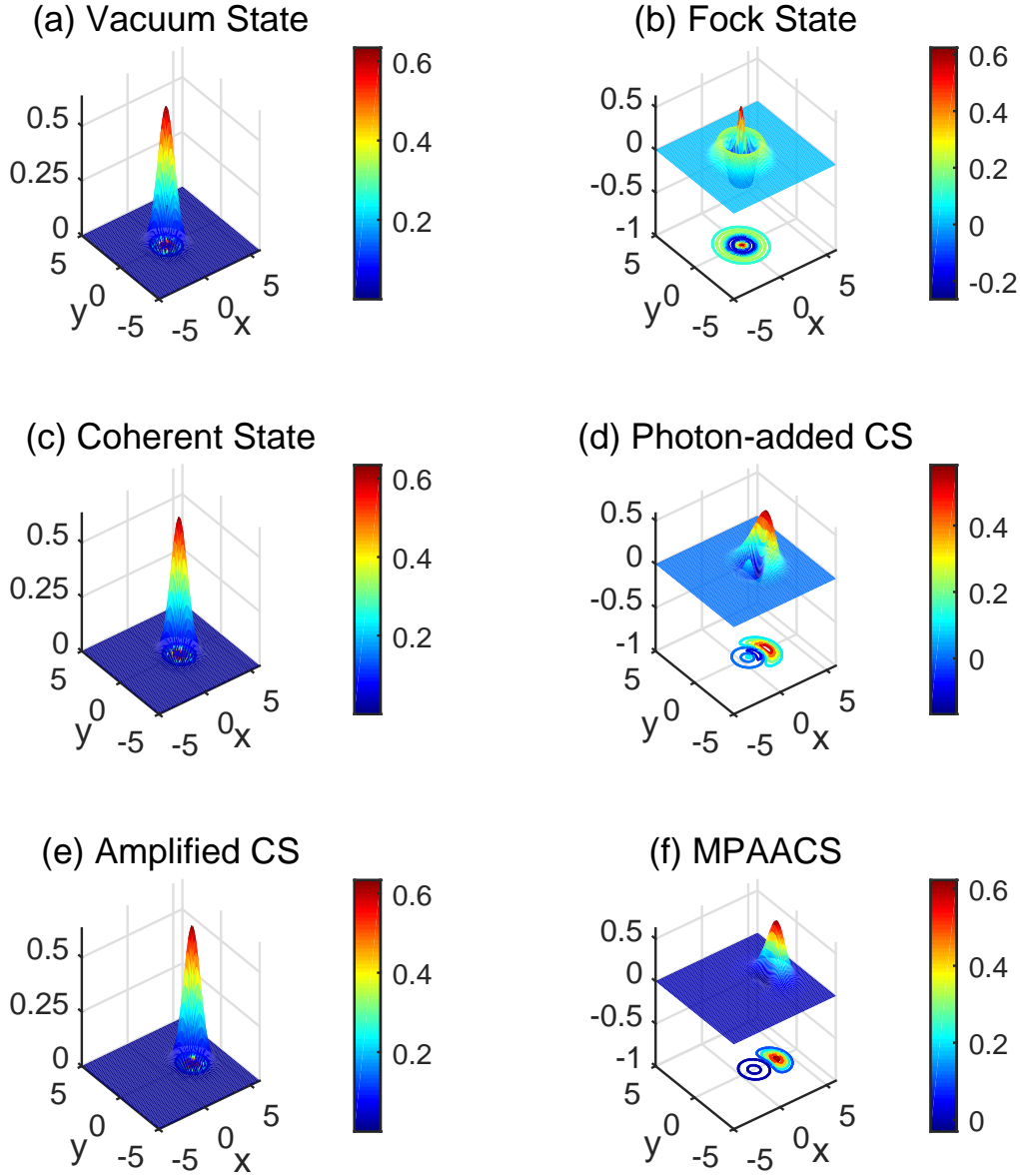


FIG. 4: WFs $W(\beta)$ of $|\psi\rangle$ in the phase space (x, y) . Here, $|\psi\rangle = (|\alpha\rangle, g, m)$ are taking (a) $|0\rangle - (0, 1, 0)$; (b) $|m\rangle - (0, 1, 2)$; (c) $|\alpha\rangle - (1, 1, 0)$; (d) $a^{\dagger m} |\alpha\rangle - (1, 1, 2)$; (e) $|g\alpha\rangle - (1, 2, 0)$; and (f) $a^{\dagger m} |g\alpha\rangle - (1, 2, 2)$.

which tells how much noise has been added to the input noise level. In fact, the EIN came from a classical electronics terminology and used to quantify the performance of an amplifier[27, 28, 32, 33]. For an amplification process, the EIN is negative and indicates the characteristic of noiseless amplification[34].

In Fig.6(c), the EINs are shown as a function of $|\alpha|$ for $|\psi\rangle$ with different g and m . The numerical results

reveal that N_{eq} is clearly negative for all $|\alpha|$, except case $m = 0$ and $g = 1$. The main results include: (1) For $m = 0$, we know that N_{eq} remains constant $0.5/g^2 - 0.5$ for any g and all $|\alpha|$; (2) In the limit of $|\alpha| \rightarrow 0$, we see $N_{eq} \rightarrow 0.5/g^2 - 0.5$ for $m = 0$, $0.375/g^2 - 0.5$ for $m = 1$, $0.277778/g^2 - 0.5$ for $m = 2$, respectively; (3) In the limit of $|\alpha| \rightarrow \infty$, we see $N_{eq} \rightarrow 0.5/g^2 - 0.5$ for any $g (> 1)$ and different m ; (4) A minimum value of N_{eq} can be see

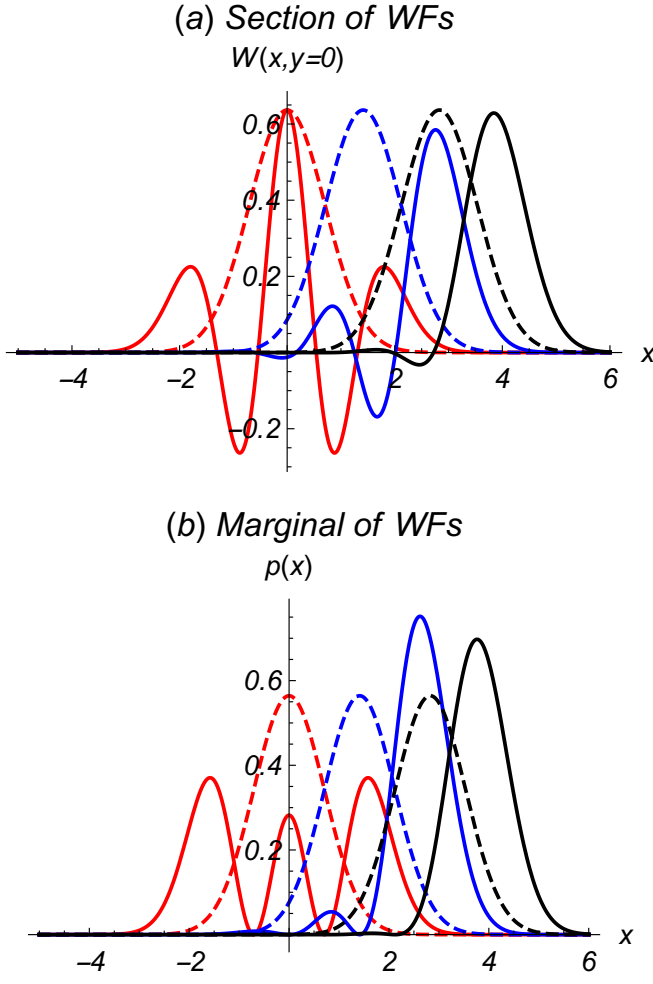


FIG. 5: (a) Sections $W(x, y = 0)$ and (b) Marginal distribution $p(x)$ of $W(\beta)$ for $|\psi\rangle$ in Fig.4 as a function of x . Here, $|\psi\rangle$ - $(|\alpha\rangle, g, m)$ taking (red dashed) $|0\rangle$ - $(0, 1, 0)$; (red solid) $|m\rangle$ - $(0, 1, 2)$; (blue dashed) $|\alpha\rangle$ - $(1, 1, 0)$; (blue solid) $a^{\dagger m}|\alpha\rangle$ - $(1, 1, 2)$; (black dashed) $|g\alpha\rangle$ - $(1, 2, 0)$; and (black solid) $a^{\dagger m}|g\alpha\rangle$ - $(1, 2, 2)$.

at proper $|\alpha|$ for each case.

VI. CONCLUSION AND DISCUSSION

We have introduced MPAACSs by applying AM $g^{\hat{n}}$ and AD $\hat{a}^{\dagger m}$ on $|\alpha\rangle$ and proved that state $g^{\hat{n}}\hat{a}^{\dagger m}|\alpha\rangle$ and state $\hat{a}^{\dagger m}g^{\hat{n}}|\alpha\rangle$ are state $\hat{a}^{\dagger m}|g\alpha\rangle$. From $|\alpha\rangle$ to $\hat{a}^{\dagger m}|g\alpha\rangle$, the combinatorial effect of $g^{\hat{n}}$ and $\hat{a}^{\dagger m}$ is working as an amplifier. From the point of view of quantum state engineering, these MPAACSs $\hat{a}^{\dagger m}|g\alpha\rangle$ are a class of new quantum states, which include many familiar quantum states, such as $|0\rangle$, $|m\rangle$, $|\alpha\rangle$, $|g\alpha\rangle$, and $\hat{a}^{\dagger m}|g\alpha\rangle$. We have derived the normalization factor for the MPAACS and found that it is related to Laguerre polynomials. Interesting physical properties are given analytically and simulated numerically according to the supplementary materials. The main results are summarized as follows.

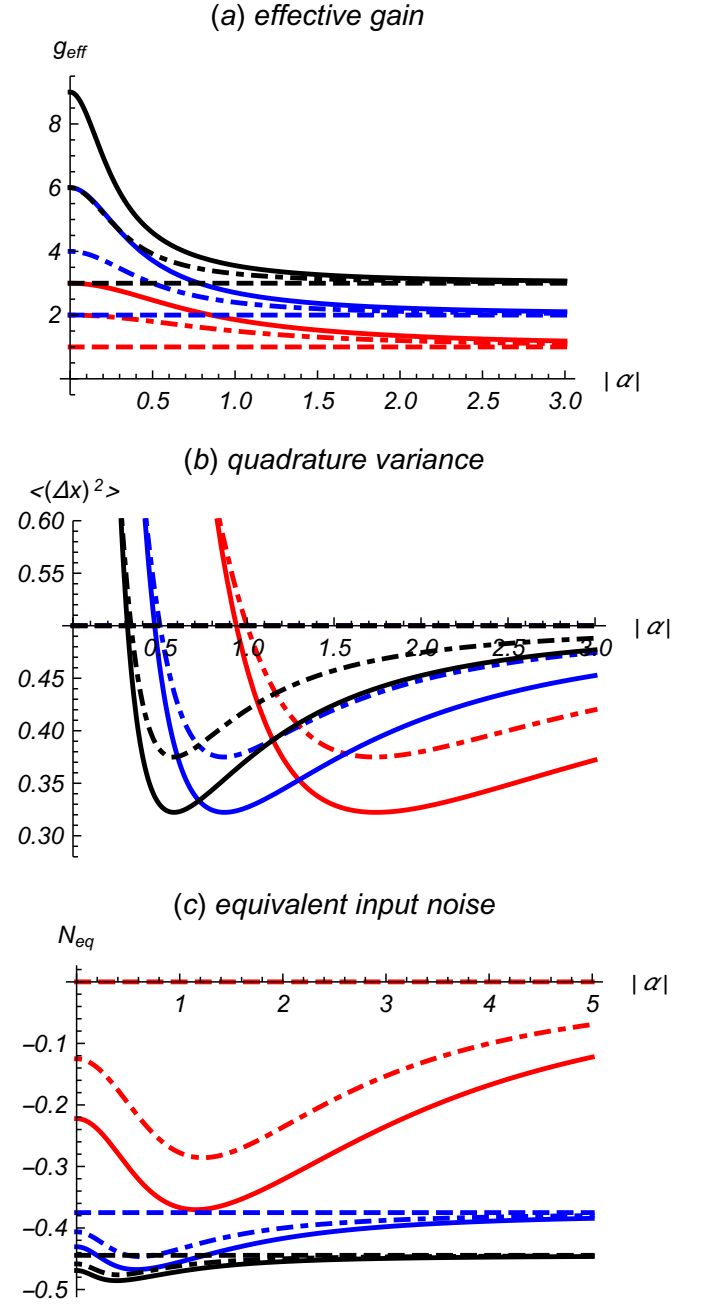


FIG. 6: (a) Effective gain g_{eff} , (b) Variances $\langle(\Delta x)^2\rangle$, and (c) Equivalent input noise N_{eq} as the function of $|\alpha|$. Here, parameters are taking $g = 1$ (red), 2 (blue), 3 (black) and $m = 0$ (dashed), 1 (dotdashed), 2 (solid).

As for the effects of AM $g^{\hat{n}}$ and AD $\hat{a}^{\dagger m}$ on photon components of the MPAACSs, we find that: (1) The AD $\hat{a}^{\dagger m}$ leads to the void of the low-photon components (including $|0\rangle$, $|1\rangle$, \dots , $|m-1\rangle$) and the re-layout of photon components. (2) The AM $g^{\hat{n}}$ leads to the re-layout of photon components. As for the effects of AM $g^{\hat{n}}$ and AD $\hat{a}^{\dagger m}$ on WFs, we find that: (1) The AD $\hat{a}^{\dagger m}$ is a non-Gaussian operation, which can transform a Gaussian state into a non-gaussian state, accompanying with

Wigner negativity. (2) The AM $g^{\hat{n}}$ is a Gaussian operation, which can remain original Gaussianity or non-Gaussianity of quantum state. As for the effects of AM $g^{\hat{n}}$ and AD $\hat{a}^{\dagger m}$ on amplification, squeezing and noise, we find that: (1) Both $g^{\hat{n}}$ and $\hat{a}^{\dagger m}$ can improve the effective gain by changing g and m . (2) The quadrature squeezing will exhibit when $|g\alpha|$ exceeds a certain threshold except $m = 0$. (3) The EINs except case $g = 1$ and $m = 0$ are negative, showing the characteristic of noiseless amplification.

In our previous works[35–37], we have introduced several amplified quantum states, such as amplified coherent state, amplified thermal state, and amplified squeezed vacuum, by applying $(g-1)\hat{n} + 1$ or $(g - \sqrt{2g-1})\hat{n}^2 + (\sqrt{2g-1}-1)\hat{n} + 1$ on the corresponding input states. These amplified states can exhibit their respective peculiar nonclassicality. Of course, these operators work as amplifiers of realizing signal amplification. However, it is actually impossible to implement a perfect noiseless amplifier described by $g^{\hat{n}}$, albeit with zero success probability[38]. So, our present work only provides a theoretical reference for signal amplification in quantum technology or state generation in quantum state engineering.

Appendix: Supplemental Materials

Using techniques such as $g^{\hat{n}} =: e^{(g-1)\hat{a}^{\dagger}\hat{a}} : (\dots : \text{denotes normal ordering})$ and $x^n = \partial_s^n e^{sx}|_{s=0}$, we provide the following supplemental materials for all informations discussed in the main text.

Appendix A: Information for state $|\psi_1\rangle$

In this appendix, we provide the state description, normalization, expectation value, density matrix elements and Wigner function for $|\psi_1\rangle$.

(a) State description

Eq.(1) can be further written as

$$|\psi_1\rangle = \frac{e^{-\frac{|\alpha|^2}{2}}}{\sqrt{N_1}} \partial_{s_1}^m e^{g(\alpha+s_1)a^\dagger} |0\rangle |_{s_1=0}, \quad (\text{A.1})$$

accompanying with conjugate state

$$\langle\psi_1| = \frac{e^{-\frac{|\alpha|^2}{2}}}{\sqrt{N_1}} \partial_{t_1}^m \langle 0| e^{g(\alpha^*+t_1)a} |_{t_1=0}, \quad (\text{A.2})$$

which leads to density operator $\rho_1 = |\psi_1\rangle \langle\psi_1|$,

$$\rho_1 = \frac{e^{-|\alpha|^2}}{N_1} \partial_{s_1}^m \partial_{t_1}^m e^{g(\alpha+s_1)a^\dagger} |0\rangle \langle 0| e^{g(\alpha^*+t_1)a} |_{(s_1,t_1)=0}. \quad (\text{A.3})$$

(b) Normalization

The normalization factor is

$$N_1 = e^{(g^2-1)|\alpha|^2} \partial_{s_1}^m \partial_{t_1}^m e^{g^2(t_1\alpha+s_1\alpha^*+s_1t_1)} |_{(s_1,t_1)=0}. \quad (\text{A.4})$$

Using the following formula

$$L_m(xy) = \frac{(-1)^m}{m!} \partial_s^m \partial_t^m e^{-st+sx+ty} |_{(s,t)=0}, \quad (\text{A.5})$$

we easily obtain the analytical result of N_1 in Eq.(2).

(c) Expectation value

Here, we give $\langle a^{\dagger k} a^l \rangle_{\rho_1}$ as follows

$$\begin{aligned} \langle a^{\dagger k} a^l \rangle_{\rho_1} &= \frac{e^{(g^2-1)|\alpha|^2}}{N_1} \partial_{s_1}^m \partial_{t_1}^m \partial_{f_1}^k \partial_{h_1}^l \\ &\quad e^{g(h_1\alpha+f_1\alpha^*)+g^2(t_1\alpha+s_1\alpha^*+s_1t_1)} \\ &\quad e^{g(h_1s_1+f_1t_1)} |_{(s_1,t_1,f_1,h_1)=0}. \end{aligned} \quad (\text{A.6})$$

(d) Density matrix elements

Here, we give $\rho_{kl}^{(1)} = \langle k|\rho_1|l\rangle$ with the following form

$$\begin{aligned} \rho_{kl}^{(1)} &= \frac{e^{-|\alpha|^2}}{N_1 \sqrt{k!l!}} \partial_{s_1}^m \partial_{t_1}^m \partial_{f_1}^k \partial_{h_1}^l \\ &\quad e^{gf_1(\alpha+s)+gh_1(\alpha^*+t)} |_{(s_1,t_1,f_1,h_1)=0}. \end{aligned} \quad (\text{A.7})$$

(e) Wigner function

WF of ρ_1 has the following form

$$\begin{aligned} W_{\rho_1}(\beta) &= \frac{2}{\pi N_1} e^{-(g^2+1)|\alpha|^2-2|\beta|^2+2g\alpha\beta^*+2g\alpha^*\beta} \\ &\quad \partial_{s_1}^m \partial_{t_1}^m e^{-g^2(t_1\alpha+s_1\alpha^*+s_1t_1)+2g(t_1\beta+s_1\beta^*)} |_{(s_1,t_1)=0} \end{aligned} \quad (\text{A.8})$$

Appendix B: Information for state $|\psi_2\rangle$

In this appendix, we provide the state description, normalization, expectation value, density matrix elements and Wigner function for $|\psi_2\rangle$.

(a) State description

Eq.(3) can be further written as

$$|\psi_2\rangle = \frac{e^{-\frac{|\alpha|^2}{2}}}{\sqrt{N_2}} \partial_{s_2}^m e^{(s_2+g\alpha)a^\dagger} |0\rangle |_{s_2=0}, \quad (\text{B.1})$$

accompanying with conjugate state

$$\langle\psi_2| = \frac{e^{-\frac{|\alpha|^2}{2}}}{\sqrt{N_2}} \partial_{t_2}^m \langle 0| e^{(t_2+g\alpha^*)a} |_{t_2=0}, \quad (\text{B.2})$$

and leads to density operator $\rho_2 = |\psi_2\rangle \langle\psi_2|$,

$$\rho_2 = \frac{e^{-|\alpha|^2}}{N_2} \partial_{s_2}^m \partial_{t_2}^m e^{(s_2+g\alpha)a^\dagger} |0\rangle \langle 0| e^{(t_2+g\alpha^*)a} |_{(s_2,t_2)=0}. \quad (\text{B.3})$$

(b) Normalization

The normalization factor is

$$N_2 = e^{(g^2-1)|\alpha|^2} \partial_{s_2}^m \partial_{t_2}^m e^{gt_2\alpha+gs_2\alpha^*+s_2t_2} |_{(s_2,t_2)=0}, \quad (\text{B.4})$$

which leads to the analytical result of N_2 in Eq.(4).

(c) Expectation value

Here, we give $\langle a^{\dagger k} a^l \rangle_{\rho_2}$ as follows

$$\langle a^{\dagger k} a^l \rangle_{\rho_2} = \frac{e^{(g^2-1)|\alpha|^2}}{N_2} \partial_{s_2}^m \partial_{t_2}^m \partial_{f_2}^k \partial_{h_2}^l e^{g(h_2+t_2)\alpha+g(f_2+s_2)\alpha^*} e^{h_2 s_2 + f_2 t_2 + s_2 t_2} \Big|_{(s_2, t_2, f_2, h_2)=0}. \quad (\text{B.5})$$

(d) Density matrix elements

Here, we give $\rho_{kl}^{(2)} = \langle k | \rho_2 | l \rangle$ with the following form

$$\rho_{kl}^{(2)} = \frac{e^{-|\alpha|^2}}{N_2 \sqrt{k!l!}} \partial_{s_2}^m \partial_{t_2}^m \partial_{f_2}^k \partial_{h_2}^l e^{f_2 s_2 + h_2 t_2 + g(f_2 \alpha + h_2 \alpha^*)} \Big|_{(s_2, t_2, f_2, h_2)=0}. \quad (\text{B.6})$$

(e) Wigner function

WF of ρ_2 has the following form

$$W_{\rho_2}(\beta) = \frac{2}{\pi N_2} e^{-(g^2+1)|\alpha|^2 - 2|\beta|^2 + 2g(\alpha\beta^* + \alpha^*\beta)} \partial_{s_2}^m \partial_{t_2}^m e^{-g(t_2\alpha + s_2\alpha^*) - s_2 t_2 + 2(t_2\beta + s_2\beta^*)} \Big|_{(s_2, t_2)=0} \quad (\text{B.7})$$

Acknowledgments

This project was supported by the National Natural Science Foundation of China (No. 11665013).

-
- [1] C. M. Caves, Quantum limits on noise in linear amplifiers, *Phys. Rev. D* 26, 1817-1839 (1982).
- [2] W. K. Wootters and W. H. Zurek, A single quantum cannot be cloned, *Nature Photon.* 299, 802-803 (1982).
- [3] V. Scarani, S. Iblisdir, N. Gisin and A. Acin, Quantum cloning, *Rev. Mod. Phys.* 77, 1225-1256 (2005).
- [4] D. Bruss, G. M. D'Ariano, C. Macchiavello, and M. F. Sacchi, Approximate quantum cloning and the impossibility of superluminal information transfer, *Phys. Rev. A* 62, 062302 (2000).
- [5] T. C. Ralph and A. P. Lund, Nondeterministic noiseless linear amplification of quantum systems, *AIP Conf. Proc.* 1110, 155-160 (2000).
- [6] J. Fiurasek, Optimal linear-optical noiseless quantum amplifiers driven by auxiliary multiphoton Fock states, *Phys. Rev. A* 105, 062425 (2022).
- [7] M. Barbieri, F. Ferreyrol, R. Blandino, R. Tualle-Brouiri, and Ph. Grangier, Nondeterministic noiseless amplification of optical signals: a review of recent experiments, *Laser Phys. Lett.* 8(6), 411-417 (2011).
- [8] G. Y. Xiang, T. C. Ralph, A. P. Lund, N. Walk, and G. J. Pryde, Heralded noiseless linear amplification and distillation of entanglement, *Nature Photon.* 4, 316-319 (2010).
- [9] A. Karsa, M. Ghalaii, and S. Pirandola, Noiseless linear amplification in quantum target detection using Gaussian states, *Quantum Sci. Technol.* 7, 035026 (2022).
- [10] J. Fiurasek, Teleportation-based noiseless quantum amplification of coherent states of light, *Opt. Exp.* 30, 1466-1489 (2022).
- [11] M. Micuda, I. Straka, M. Mikova, M. Dusek, N. J. Cerf, J. Fiurasek, and M. Jezek, Noiseless loss suppression in quantum optical communication, *Phys. Rev. Lett.* 109, 180503 (2012).
- [12] J. Dias and T. C. Ralph, Quantum repeaters using continuous-variable teleportation, *Phys. Rev. A* 95, 022312 (2017).
- [13] T. C. Ralph, Quantum error correction of continuous-variable states against Gaussian noise, *Phys. Rev. A* 84, 022339 (2011).
- [14] Y. Liu, K. M. Zheng, H. J. Kang, D. M. Han, M. H. Wang, L. J. Zhang, X. Su, and K. C. Peng, Distillation of Gaussian Einstein-Podolsky-Rosen steering with noiseless linear amplification, *npj Quantum Inf.* 8, 38 (2022).
- [15] J. Fiurasek, Engineering quantum operations on traveling light beams by multiple photon addition and subtraction, *Phys. Rev. A* 80, 053822 (2009).
- [16] C. N. Gagatsos, J. Fiurasek, A. Zavatta, M. Bellini, and N. J. Cerf, Heralded noiseless amplification and attenuation of non-Gaussian states of light, *Phys. Rev. A* 89, 062311 (2014).
- [17] J. Park, J. Joo, A. Zavatta, M. Bellini, and H. Jeong, Efficient noiseless linear amplification for light fields with larger amplitudes, *Opt. Exp.* 24, 253560 (2016).
- [18] G. S. Agarwal and K. Tara, Nonclassical properties of states generated by the excitations on a coherent state, *Phys. Rev. A* 43, 492-497 (1991).
- [19] G. Dattoli, Generalized Polynomials, Operational Identities and Their Applications, *J. Comput. Appl. Math.* 118, 111-123 (2000).
- [20] E. P. Wigner, On the Quantum Correction For Thermodynamic Equilibrium, *Phys. Rev.* 40, 794-759 (1932).
- [21] W. P. Schleich, *Quantum Optics in Phase Space*, Berlin: Wiley-VCH, 2001.
- [22] K. E. Cahill and R. J. Glauber, Density operators and quasiprobability distributions, *Phys. Rev.* 177, 1882-1902 (1969).
- [23] A. Kenfack and K. Życzkowski, Negativity of the Wigner function as an indicator of non-classicality, *J. Opt. B: Quantum Semiclass. Opt.* 6, 396 (2004).
- [24] V. Cimini, M. Barbieri, N. Treps, M. Walschaers, and V. Parigi, Neural networks for detecting multimode Wigner negativity, *Phys. Rev. Lett.* 125, 160504 (2020).
- [25] M. O. Scully and M. S. Zubairy, *Quantum Optics*, Cambridge University Press, 1997.
- [26] X. X. Xu and H. C. Yuan, Generating single-photon catalyzed coherent states with quantum-optical catalysis, *Phys. Lett. A* 380, 2342-2348 (2016).
- [27] F. Ferreyrol, M. Barbieri, R. Blandino, S. Fossier, R. Tualle-Brouiri, and P. Grangier, Implementation of a Nondeterministic Optical Noiseless Amplifier, *Phys. Rev. Lett.* 104, 123603 (2010).
- [28] A. Zavatta, J. Fiurasek, and M. Bellini, A high-fidelity noiseless amplifier for quantum light states, *Nature Pho-*

- ton. 5, 52-56 (2011).
- [29] C. C. Gerry and P. L. Knight, *Introductory Quantum Optics*, Cambridge University Press, 2005.
- [30] D. F. Walls, Squeezed states of light, *Nature* 306, 141-146 (1983).
- [31] A. Zavatta, S. Viciani, and M. Bellini, Single-photon excitation of a coherent state: Catching the elementary step of stimulated light emission, *Phys. Rev. A* 72, 023820 (2005).
- [32] J. R. Roch, J. Ph. Poizat, and P. Grangier, Sub-shot-noise manipulation of light using semiconductor emitters and receivers, *Phys. Rev. Lett.* 71, 2006 (1993).
- [33] F. Grosshans, G. Van Assche, J. Wenger, R. Brouri, N. J. Cerf, and P. Grangier, Quantum key distribution using Gaussian-modulated coherent states, *Nature* 421, 238-241 (2003)
- [34] J. Park, J. Joo, A. Zavatta, M. Bellini, and H. Jeong, Efficient noiseless linear amplification for light fields with larger amplitudes, *Opt. Express* 24, 253560 (2016).
- [35] Y. B. Cheng, S. G. Guan, Z. J. Wang and X. X. Xu, Comparative analysis of properties for amplified coherent state and amplified squeezed vacuum, *Mod. Phys. Lett. B* 34, 2050377 (2020)
- [36] Q. Ke, Y. F. Wang, Y. B. Cheng, and X. X. Xu, Signal characters and non-classical properties of quadratically amplified squeezed vacuum, *Mod. Phys. Lett. B* 35, 2150028 (2021)
- [37] Z. Y. Zhao and X. X. Xu, Amplified thermal state: Properties and decoherence, *Mod. Phys. Lett. B* 35, 2150448 (2021).
- [38] C. N. Gagatsos, E. Karpov, and N. J. Cerf, Probabilistic phase-insensitive optical squeezer in compliance with causality, *Phys. Rev. A* 86, 012324 (2012).